

## Electrical probing of endothelial cell behaviour on a fibronectin/polystyrene/thiol/gold electrode by Faradaic electrochemical impedance spectroscopy (EIS)

Amira Bouafsoun<sup>a,b</sup>, Saloua Helali<sup>a</sup>, Saida Mebarek<sup>d</sup>, Caroline Zeiller<sup>d</sup>, Annie-France Prigent<sup>d</sup>, Ali Othmane<sup>b</sup>, Abdelhamid Kerkeni<sup>b</sup>, Nicole Jaffr  zic-Renault<sup>a,\*</sup>, Laurence Ponsonnet<sup>c</sup>

<sup>a</sup> CEGELY, UMR-CNRS 5005,   cole Centrale de Lyon, 69134   cully Cedex - France

<sup>b</sup> Laboratoire de Biophysique, Facult   de M  decine de Monastir-5019 Monastir-Tunisia

<sup>c</sup> Laboratoire des Polym  res, Biopolym  res et Membranes (PBM) - Universit   de Rouen-76 821 Mont Saint-Aignan Cedex - France

<sup>d</sup> Laboratoire de physiopathologie des lipides et des membranes - INSERM 585, B  timent Louis Pasteur, INSA de Lyon-69621 Villeurbanne, France

Received 22 November 2005; received in revised form 23 May 2006; accepted 29 May 2006

Available online 3 June 2006

### Abstract

The electrochemical impedance spectroscopy (EIS) technique has been shown to be an effective tool for monitoring endothelial cell behaviour on a multilayer functionalised gold electrode. Polystyrene, a reproducible model substrate, is deposited as a thin layer on a thiol functionalised gold electrode. Fibronectin, a protein promoting endothelial cell adhesion, is then adsorbed on the polystyrene surface. The different steps of this multilayer assembly are characterized by Faradaic impedance. The charge transfer resistance and the capacitance for the total layer are modified at each step according to the electrical properties of each layer. This gives the endothelial cells' electrical state in terms of its resistive and capacitive properties. In this study, the endothelial cell layer presents a specific charge transfer resistance equal to  $1.55 \text{ k}\Omega \text{ cm}^2$  with no large defects in the cell layer, and a specific capacitance equal to few  $\mu\text{F cm}^{-2}$  explained by the existence of pseudopods. These electrical properties are correlated to the endothelial cell viability, adhesion and cytoskeleton organization.

   2006 Elsevier B.V. All rights reserved.

**Keywords:** Electrochemical Impedance Spectroscopy (EIS); Endothelial cell; Fibronectin; Polystyrene

### 1. Introduction

By virtue of its unique location in the vessel wall, the endothelium constitutes an essential interface. It is important to characterize endothelial cell adhesion to be able to predict and control the outcome of the interaction between artificial surfaces and living cells, so that biomedical devices of antithrombogenic vascular grafts can be developed. Polystyrene was chosen because it constitutes a reproducible model substrate were often used for the study of cell–material interactions [1]. In order to promote cell adhesion, fibronectin is firstly adsorbed [2]. Methods which enable the rapid analysis of endothelial barrier properties are becoming

widespread and attracting growing interest. The technique adopted in this paper is Faradaic electrochemical impedance spectroscopy (EIS) which is a sensitive indicator of chemical and physical interactions at the solid/liquid interfaces. It combines the analysis of both the resistive and capacitive properties of solid/liquid interfaces, based on the perturbation of a system at equilibrium by a sinusoidal excitation signal of small amplitude. The potential of EIS is that the system can be scanned over a wide range of alternative potential frequencies. The corresponding circuit models are useful for the interpretation of impedance spectra. There is an increasing trend towards the development of impedimetric biosensors [3]. When cells are grown on an electrode, electrical impedance measurements allow the characterization of the biological system. This method could provide information on the cell membranes, junction resistance, the extracellular matrix structure (ECM), and the interface structure [4]. Many studies have been performed on cultures of endothelial cells to investigate

\* Corresponding author. Postal address: Ecole Centrale de Lyon, Laboratoire CEGELY, 36 Avenue Guy de Collongue, 69134 Ecully, Lyon, France. Tel.: +33 4 72 18 62 43; fax: +33 4 78 43 37 17.

E-mail address: [nicole.jaffrezic@ec-lyon.fr](mailto:nicole.jaffrezic@ec-lyon.fr) (N. Jaffr  zic-Renault).

their electrical properties as a function of temperature, toxic agents or even contact with cancer cells. Giaever et al. introduced impedance spectroscopy in order to investigate cell motion and to study the electrical properties of epithelial cell monolayers in real time on a solid support. Furthermore, they presented a theoretical model for the impedance characteristics of a cell-covered gold electrode. However, these authors predominantly analysed the impedance of a cell-covered gold electrode at one defined frequency in order to observe impedance fluctuations due to vertical movements of the cells. This impedance technique is referred to as electrical cell-substrate impedance sensor (ECIS) [5–8]. Ehret et al. used impedance measurements on interdigitated electrodes to monitor the concentration, growth and physiological state of cells in culture [9]. Wegner et al. studied the effect of  $\beta$ -adrenergic hormones on bovine aortic endothelial cell monolayers grown on a gold-film-covered glass substrate. They interpreted the impedance in terms of two different contributions to the electrical resistance of cell monolayers: (i) the ion permeability of the intercellular space between adjacent cells; (ii) the conductivity of the narrow space between the cell monolayer and the substrate. Moreover, it was postulated that the capacitance of the confluent endothelial cell monolayer is determined by the apical and basal membranes. The application of agonists was shown to lead to an increase of the cell monolayer resistance, while the capacitance remains unaffected [10].

In this work, the samples characterised by Faradaic electrochemical impedance spectroscopy were previously controlled by a cytotoxicity test, adherence assay and cytoskeleton staining to investigate the endothelial cell viability, adhesion and morphology. The purpose of this study is to determine if the EIS technique senses the different layers deposited on a gold electrode, and to correlate the interface's electrical properties to the cell viability and adherence to the substrate.

## 2. Experimental

### 2.1. Material

Octadecylmercaptan  $\text{CH}_3(\text{CH}_2)_{17}\text{SH}$  was purchased from Sigma–Aldrich. The M199 medium, foetal serum (SVF), L-glutamine, penicillin-streptomycin, fibronectin, polystyrene (PS) and trypsin-EDTA were obtained from Sigma. The electrolyte used for all the experiments was a complete cell culture medium, pH=7.8 containing the redox couple  $\text{Fe}(\text{CN})_6^{3-}/\text{Fe}(\text{CN})_6^{4-}$  at a 5 mM concentration. All reagents were of analytical grade and ultrapure water (resistance  $18.2 \text{ M}\Omega \text{ cm}^{-1}$ ) produced by a Millipore Milli-Q system was used throughout.

### 2.2. Fabrication and pretreatment of gold substrate

Gold substrates were provided by the Laboratoire d'Analyse et d'Architecture des Systèmes (LAAS), CNRS Toulouse. They were fabricated using standard silicon technologies. (100)-oriented, P-type (3–5  $\Omega\text{cm}$ ) silicon wafers were thermally oxidized to grow a 800 nm-thick field oxide. Then, a 30 nm-thick titanium layer and a 300 nm-thick gold top layer were deposited by evaporation under vacuum.

Before use, the gold substrates were cleaned with acetone in an ultrasonic bath for 10 min and dried under nitrogen flow, followed by immersion in a Pirhana solution (7:3 v/v,  $\text{H}_2\text{SO}_4$ :  $\text{H}_2\text{O}_2$ ) for 1 min in order to get rid of inorganic and organic contaminants on the substrate surface. They were subsequently rinsed thoroughly in absolute ethanol and finally dried under nitrogen flow.

### 2.3. Preparation of self-assembled monolayers

After cleaning, the gold electrodes were immediately immersed in an ethanol solution of 2 mM of Octadecylmercaptan  $\text{CH}_3(\text{CH}_2)_{17}\text{SH}$  for 21 h at room temperature. After the formation of the monolayer, the substrate was rinsed 4 to 5 times with ethanol and dried under a  $\text{N}_2$  flow. Then, the substrates were immediately immersed in a polystyrene (molecular weight: 200) solution for 2 h. Once lyophilised human fibronectin had been reconstituted in a sterile buffer solution saline at 1 mg/l, the samples were coated with fibronectin solution for 2 h at room temperature.

### 2.4. Cell experiments

#### 2.4.1. Cell culture

Endothelial cells were obtained from a line (Eahy 926) and were grown in Medium 199 supplemented with 10% SVF, 2 mmol/l glutamine, 100 U/ml penicillin and 100  $\mu\text{g}/\text{ml}$  streptomycin [11]. Cultures were incubated at 37 °C in a humidified atmosphere containing 5%  $\text{CO}_2$ . Replicated cultures were obtained by trypsinization and were used for passages <5 [12]. The endothelial cell identification was confirmed by their polygonal morphology. The endothelial cells were cultured onto substrates prepared for the impedance experiments. Cell cultures were also performed on other substrates composed of glass functionalized by octadecyltrichlorosilane ( $\text{CH}_3$  terminal groups) and activated by polystyrene prepared for viability studies, actin staining and adhesion tests. In both series of experiments the model PS/fibronectin interface is the same, the glass system, being transparent, is therefore adapted to the microscopic assays.

#### 2.4.2. Cell colorimetric assay: MTT test

A converting MTT Kit (Roche, 145007) was used to assess the viability of the cultured cells. The assay is based on the cleavage of the yellow tetrazolium salt MTT to purple formazan crystals by active metabolic cells. The formazan crystals were rendered soluble. This cellular reduction involves the pyridine nucleotide cofactors NADH and NADPH. Endothelial cells were resuspended in the medium at a concentration of  $2 \times 10^5$  cells/ml and incubated overnight at 37° under humidified atmosphere containing 5%  $\text{CO}_2$ . The cells were treated with the MTT Kit for 4 h. The formazan salt crystals were formed, and were then rendered soluble by adding the solution (10% SDS in 0.01 M HCl). The resulting colored solution was quantified by a scanning multiwell spectrophotometer (Powerwave X, Biotek instruments INC) using a test wavelength of 570 nm and a reference wavelength of 690 nm [13].

#### 2.4.3. Actin filament immunofluorescent staining

After 24 h of culture in BSA medium, the cells were fixed with 3.7% formaldehyde for 10 min, rendered permeable with 0.25% Triton X-100 for 15 min, and a specific labelling was blocked in 1% BSA for 20 min. After extensive washing, rhodamin phalloidin (Molecular Probes R415) was added 1:200 diluted in PBS. The stained cells were viewed using a Zeiss fluorescence microscope (Axiovert 200 M) [14,15].

#### 2.4.4. Cell attachment assay

The number of endothelial cells attached to different substrates was assessed by staining and counting nuclei. In order to label the endothelial cell nuclei, we proceeded as described above for the fixation and the permeabilization steps. The endothelial cells seeded on different substrates were incubated with 4', 6-diamidino-2-phenylindole, dihydrochloride (DAPI) (Molecular Probes D1306) and then washed with PBS. The stained nuclei were viewed on a Zeiss fluorescence microscope and their images were analyzed with the AxioVision LE program.

#### 2.4.5. Impedance spectroscopy

The measurement set-up for impedance consisted of a classical three-electrode system, where the modified gold electrode ( $0.21 \text{ cm}^2$ ) was used as a working electrode, a platinum plate ( $0.54 \text{ cm}^2$ ) as a counter electrode and a saturated calomel electrode (SCE) as the reference electrode. The impedance analysis was performed with a Voltalab 80 impedance analyser in the frequency range 1 Hz–100 kHz, using a modulation voltage of 10 mV. During measurements the potential was kept at  $-400 \text{ mV}$ . The Faradaic impedance measurements and cyclic voltammetry measurements were performed in the presence of a  $5 \text{ mM K}_3[\text{Fe}(\text{CN})_6]/\text{K}_4[\text{Fe}(\text{CN})_6]$  (1:1) mixture as redox probe in culture medium. All electrochemical measurements were carried out at room temperature and in a Faraday cage. The Zview modelling programme (Scribner and associates, Charlottesville, VA) was used to analyse impedance data.

### 3. Results and discussion

#### 3.1. Surface modification of gold

Self-assemblies of organic molecules have been most extensively studied because of their stability, well-packed structure and versatility. One of the most widely-used systems in the molecular self-assembled method is the chemisorption of sulfur derivatives (thiols) on a gold surface, due to the thermodynamically favorable formation of the gold–thiol bonding. The stability of the bonding over a wide range of applied potentials makes this system suitable for electrochemical purposes [16]. The thiol is chemisorbed on the gold electrode and it is used as the base interface for the deposition of different layers. It has a  $\text{CH}_3$  terminal group which is hydrophobic, which allows it to interact with the polystyrene layer. By analyzing the impedance of the cell/fibronectin/PS/thiol/gold structure, in the frequency range from 1 Hz to 100 KHz, the electrical properties of the

attached cell layer can be determined in terms of its resistive and capacitive properties. The electrolyte solution is a mixture of redox solution with the cell culture medium which contains M199 and is supplemented with serum, L-glutamine and antibiotics such as penicillin-streptomycin.

#### 3.2. Characterization of multilayers on gold with cyclic voltammetry technique

Cyclic voltammetry of an electroactive species such as  $\text{Fe}(\text{CN})_6^{4-}/\text{Fe}(\text{CN})_6^{3-}$  is a valuable tool for testing the kinetic barrier of an interface. The extent of kinetic limitation of the electron transfer process increases with the increasing thickness and decreasing defect density of the barrier. Therefore, it was decided to investigate changes in electrode behaviour after each assembly step, using these electroactive species. When an electrode surface has been modified by some materials, the electron transfer kinetics are perturbed. Fig. 1 shows cyclic voltammograms obtained after the deposition of the different layers on the gold electrode.

It is well known that long thiols can form dense, well-ordered and stable monolayers on gold, as in our case [16]. The chain length is important for the characteristics of the packing density, the intermolecular environment and the geometry of the monomolecular assemblies. Cyclic voltammetry experiments can confirm that the mixed SAM layer was successfully formed on the gold surface. When the electrode surface was modified by the addition of material, the electron transfer kinetics of  $\text{Fe}(\text{CN})_6^{4-}/\text{Fe}(\text{CN})_6^{3-}$  were perturbed.

Fig. 1 shows the cyclic voltammograms of  $\text{Fe}(\text{CN})_6^{4-}/\text{Fe}(\text{CN})_6^{3-}$  at the bare gold electrode, thiol Au-electrode, polystyrene/thiol/Au-electrode, fibronectin/polystyrene/thiol/Au-electrode and endothelial cell/fibronectin/polystyrene/thiol/Au-electrode. As shown in Fig. 1, the stepwise assembly of bare gold and SAMs is accompanied by a decrease in the peak height and an increase in the peak to peak separation between the cathodic and anodic waves of the redox probe. This shows the formation of the thiol monolayer. The addition of the further layers does not strongly

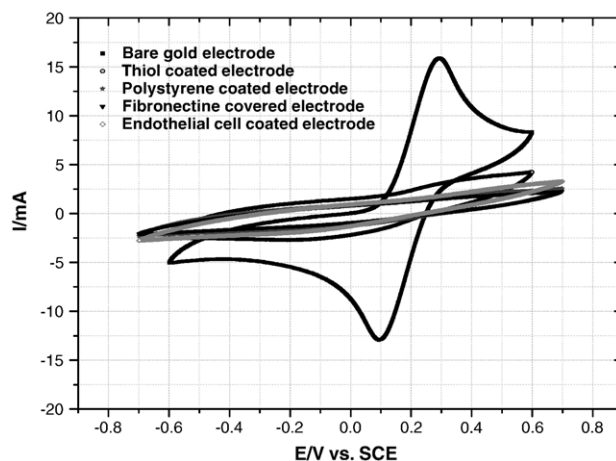


Fig. 1. Cyclic voltammetric measurement with the presence of the  $5 \text{ mM K}_3[\text{Fe}(\text{CN})_6]/\text{K}_4[\text{Fe}(\text{CN})_6]$  redox probe: bare gold electrode, thiol Au-electrode, polystyrene coated Au-electrode and fibronectin functionalized Au-electrode. All experiments were performed in culture medium pH 7.8, scan rate  $50 \text{ mV/s}$ .

modify the CV curve, showing that the electron current flowing through the biofilm is not modified by the addition of the different layers.

### 3.3. Impedance analysis of the gold electrode coated with thiol SAM, polystyrene and fibronectin

EIS of thiol/gold, polystyrene/thiol/gold and fibronectin/polystyrene/thiol/gold were investigated at a constant concentration of redox species  $\text{Fe}(\text{CN})_6^{4-/3-}$ . Typical Nyquist diagrams of the gold electrode functionalized by different layers immersed in the complete culture medium, are shown in Fig. 2. The impedance-plane plots of Fig. 2 are characterized by two distinct regions: (i) a semicircle in the higher frequency range related to the charge transfer process, (ii) an inclined line in the complex-plane impedance plot defining a Warburg region of semi-infinite diffusion of species to the modified electrode. The semicircle's diameter is equal to the charge transfer resistance,  $R_{\text{ct}}$ .

The impedance spectrum is interpreted in terms of the equivalent circuit sketched in Fig. 3. Therefore it can be analyzed using an equivalent system that consists of a charge transfer resistance ( $R_{\text{ct}}$ ) and a constant phase element (CPE) in parallel,  $W$  represents the impedance associated with diffusive ion transportation (Warburg impedance) and  $R_s$  the electrolyte solution resistance. For reason of quantifying the data, CPE is considered as a “power-law-dependent specific layer capacitance” according to:

$$\text{CPE} = A(n)^{-1} (j\omega)^{-n} \quad (1)$$

Where  $j = (-1)^{1/2}$ ,  $\omega = 2\pi f$ ,  $f$  being the frequency of the applied potential and  $A(n)$  is a constant in units  $\text{cm}^2 \text{s}^n \mu\text{F}^{-1}$ ; for  $n=1$ ,  $A(1)$  is in units  $\text{cm}^2 \text{s} \mu\text{F}^{-1}$ . The constant phase element reflects a non-homogeneity and a defect area of the layer [17–21].

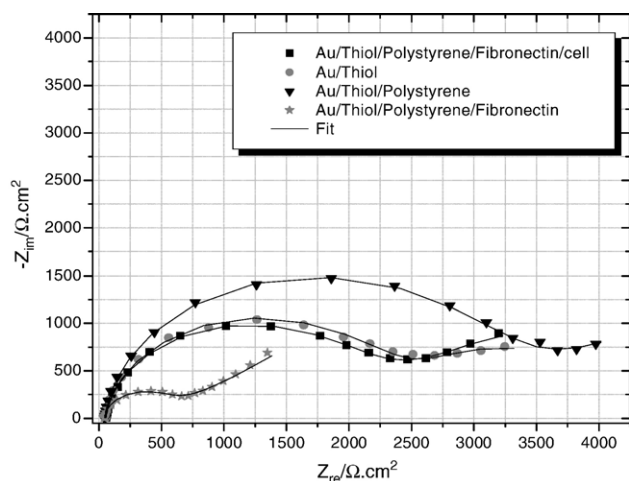


Fig. 2. Nyquist diagram ( $Z_r$  vs.  $Z_i$ ) for the impedance measurements corresponding to thiol Au-electrode, polystyrene coated Au-electrode, fibronectin functionalized Au-electrode and endothelial cell functionalized Au-electrode. All measurements were performed in a culture medium pH 7.8. Amplitude of alternating voltage is 10 mv. Symbols show the experimental data in culture medium solution. Solid curves show the computer fitting of the data using the equivalent circuits shown in Fig. 3.

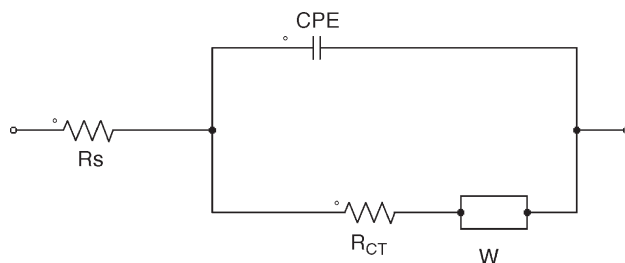


Fig. 3. Equivalent circuit used to model impedance data in culture medium.

The extent of the deviation from the Randles and Ershler model is controlled by the parameter  $n$  in Eq. (1). The CPE is a pure specific layer capacitance when  $n=1$   $\Omega \text{ cm}^2$  is the unit of the specific charge transfer layer resistance ( $R_{\text{ct}}$ ).

The experimental Faradaic impedance spectra were fitted with computer simulated spectra using the equivalent electrical circuit shown in Fig. 3. Excellent fitting between the simulated and experimental spectra was obtained for the thiol/Au electrode, the polystyrene/thiol/Au-electrode and fibronectin/polystyrene/thiol/Au-electrode (Fig. 2). It can be seen that the diameter of the semicircle at high frequency increases at each step of the formation of thiol and polystyrene layers on the electrode surface. The value of  $R_{\text{ct}}$  were extracted from the computer simulated spectra. They are  $2152 \Omega \text{ cm}^2$  and  $2800 \Omega \text{ cm}^2$  for the thiol/Au electrode and the polystyrene/thiol/Au electrode respectively. Parameter  $n$  is equal to 0.92 and 0.95 for the thiol/Au-electrode and the polystyrene/thiol/Au-electrode respectively. All these values are close to 1 which shows that CPE is essentially a specific layer capacitance. The CPE values extracted from the computer fitting for the thiol/Au electrode and the polystyrene/thiol/Au electrode were  $1.4 \mu\text{F cm}^{-2}$  and  $1.27 \mu\text{F cm}^{-2}$  respectively. The CPE decreases with the addition of the polystyrene layer, which proves that the layer thickness increases and that the polystyrene layer is directly adsorbed onto the thiol without any interpenetration of chains. If we assume a pure capacitance behaviour, the total specific capacitance of the layer can be modelled as a series of specific thiol layer capacitance and specific PS layer capacitance. If the dielectric constant of both materials is assumed to be the same ( $\epsilon=2$ ) [22] and the thickness of thiol is around 3 nm, the specific PS layer capacitance should be equal to  $13.7 \mu\text{F cm}^{-2}$  and its thickness should be 0.3 nm, corresponding to long chains laid on the thiol surface.

On the contrary, the  $R_{\text{ct}}$  decreases and CPE increases in the case of fibronectin/polystyrene/thiol/Au-electrode.  $R_{\text{ct}}$  is equal to  $554.6 \Omega \text{ cm}^2$ , even less than the  $R_{\text{ct}}$  found for thiol SAM, and CPE is equal to  $1.817 \mu\text{F cm}^{-2}$ , even higher than that found for thiol SAM. This type of electrical behaviour has already been observed when IgG is adsorbed on a mixed thiol SAM [23]. The protein itself has loops, tails, helices and sheets that can make their way through the polystyrene layer. The fibronectin has an acidic isoelectric point (pI) of (5.5–6.0). Thus the entire molecule possesses a net negative charge within the pH range of the study (7.8) so that the local ion concentration increases near the surface. Higher local ion concentrations will decrease the value of the  $R_{\text{ct}}$  and will increase the value of the dielectric constant of the biolayer leading to an increase of CPE.



### 3.4. Characterisation of endothelial cell monolayer grown on fibronectin

The histograms in Fig. 4 indicate the cell density on a substrate with and without fibronectin. The cell density increases in the presence of fibronectin treatment. Fibronectin is therefore a cell adhesion promoter. The histograms in Fig. 5 indicate the cell adhesion rates onto fibronectin, polystyrene and tissue culture polystyrene (TCPS). The corresponding percentage represents the number of adherent cells by the number of seeded cells. The results show a high endothelial cell adhesion rate on the fibronectin compared with tissue culture polystyrene (TCPS) and polystyrene. The cell density and the adhesion rate are indicators of the non-toxicity and the relatively good biocompatibility of materials activated by fibronectin. In Fig. 6, the actin filament staining shows the cobblestone form which characterizes the endothelial cell morphology. The absence of stress fibres shows the cell cytoskeleton state and reveals the cell metabolism in static conditions. Cell adhesion is qualitatively analyzed by the immune labelling of the cytoskeleton and quantitatively by the adhesion rate and the cell density. The high values of these parameters confirm the formation of an endothelial cell confluent monolayer.

### 3.5. Impedance spectra of endothelial cell monolayer grown on fibronectin

Biological cells are very poor conductors at low frequencies (at least below 10 KHz), and therefore, force electrical currents to bypass them. As cells adhere to the gold electrode, this reduces the free electrode area and increases the interface impedance [24]. The influence of cells on the impedance is plotted in Fig. 2, which presents the Nyquist diagram obtained on a confluent endothelial cell monolayer on a fibronectin/polystyrene/thiol/Au electrode.

The impedance spectrum is interpreted in terms of the equivalent circuit sketched in Fig. 3, where the  $R_{ct}$  of the modified electrode covered with endothelial cells is equal to  $2.106 \pm 0.04 \text{ k } \Omega \text{ cm}^2$ . If we assume that this value is the sum of two specific layer resistances in series—the specific resistance of

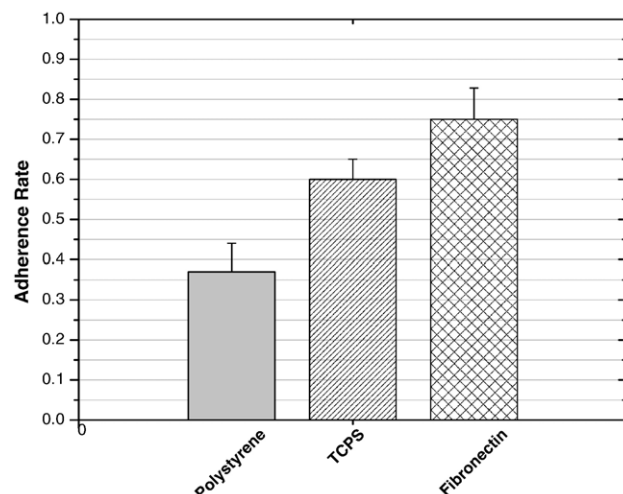


Fig. 5. Endothelial cell adhesion rate versus different substrates.

the under layer and the specific resistance of the cell layer—the specific resistance of the cell layer should be equal to  $1552 \Omega \text{ cm}^2$ .

The values for the specific cell layer resistance are consistent with literature data, considering the fact that this electrical parameter may vary over a wide range depending on the cell type and the culture medium. Rutten et al., for instance, analyzed endothelial cells initially isolated as individual clones from bovine brain microvessels. Cells of this type grown on permeable glutaraldehyde-treated collagen gels yielded specific cell layer resistances between  $160$  and  $800 \Omega \text{ cm}^2$  [25]. On the other hand, much smaller values for specific endothelial cell layer resistances were reported by Wegner et al. They obtained a value of  $30$ – $80 \Omega \text{ cm}^2$  for the porcine brain capillary endothelial cells [26] and only  $4 \Omega \text{ cm}^2$  for the bovine aortic endothelial cells [10]. Finally, for endothelial cells from brain capillary very high specific resistances of up to  $2000 \Omega \text{ cm}^2$  have been reported by Crone and Oeson [27] which is in agreement with our results. Generally, the specific resistance of cell layers is dominated by ion permeability along the intercellular clefts, because the pathway

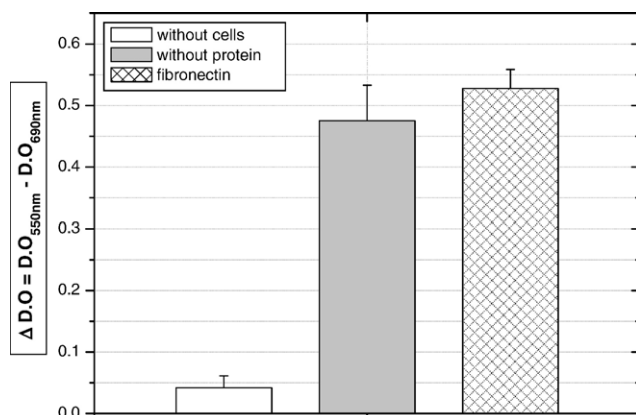


Fig. 4. Cytotoxicity test of endothelial cell grown on fibronectin.

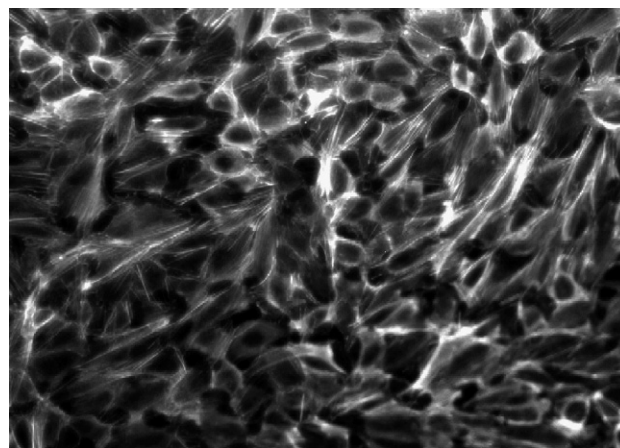


Fig. 6. Actin filament staining of endothelial cell cultured onto fibronectin with rhodamine phalloidin (Molecular Probes R415) (diluted 1:200 in PBS). The stained cells were viewed on a Zeiss fluorescence microscope (Axiovert 200 M). Bars =  $100 \mu\text{m}$ .

is expected to have much higher resistance. In addition, even the composition of the cell medium can affect the specific resistance of the layer. Turner reported a linear relationship between the reciprocal endothelial resistance and the reciprocal medium resistance, proving the existence of a mainly intercellular current [28]. Therefore, the reason for a low specific cell layer resistance may in some cases be due to defects in the confluent layer and not to real cell properties; the high specific resistance value proves that no large defects are present in the cell layer.

The specific capacitance of cell membranes is generally regarded to be approximately  $1 \mu\text{F cm}^{-2}$  [29]. Steinem et al. showed that the specific capacitance of the endothelial cell layer (porcine brain microvessel and bovine aorta) showed a value of  $0.5\text{--}0.8 \mu\text{F cm}^{-2}$  and a value of  $1\text{--}3 \mu\text{F cm}^{-2}$  for epithelial cells [30]. In this work, the  $n$  value obtained for the modified electrode covered with endothelial cells is 0.92. This value being close to 1, it shows that CPE is essentially a specific bilayer capacitance whose value is  $1.32 \mu\text{F cm}^{-2}$ . In order to deduce the value of the specific capacitance corresponding to the cell layer, it is assumed that the specific cell layer capacitance is in series with the specific underlayer capacitance ( $1.817 \mu\text{F cm}^{-2}$ ). The specific endothelial layer capacitance is then found to be equal to  $5 \mu\text{F cm}^{-2}$ . A larger specific cell layer capacitance can be explained in terms of a folding of the cell membranes and/or existence of microvilli and pseudopods [31] due to the presence of fibronectin.

#### 4. Conclusion

The interface between endothelial cell and biomaterials is interesting for the development of cardiovascular grafts. Electrochemical impedance spectroscopy (EIS) has been shown to be an effective tool for monitoring endothelial cell behaviour on a fibronectin/polystyrene/thiol/gold electrode. This method is also suitable for monitoring the interfacial properties. The specific charge transfer resistance and the specific capacitance for the total layer are modified at each step in agreement with the electrical properties of each layer. The endothelial cell layer has a specific charge transfer resistance of  $1.55 \text{ k}\Omega \text{ cm}^2$ , this high value of  $R_{ct}$  reflecting no defects in the cell layer. A specific capacitance of  $5 \mu\text{F cm}^{-2}$  is found for the cell layer which in agreement with the existence of pseudopods.

These values will be the basis of further studies oriented towards comparing the effect of other protein layers on the cell electrical properties and designing cell sensor arrays for toxic and drug detection.

#### Acknowledgements

This work was financially supported by the Rhone-Alpes Region through the MIRA Program and by the CMCU N° 05S0812.

#### References

- [1] T.G. Van Kooten, T.H. Spijker, J.H. Busscher, Plasma-treated polystyrene surfaces model surfaces for studying cell biomaterial interactions, *Biomaterials* 25 (2004) 1735–1747.
- [2] A. Bouafsoun, A. Othmane, A. Kerkeni, N. Jaffrezic-Renault, L. Ponsonnet, Evaluation of Endothelial cell adherence onto collagen and fibronectin: a comparison between jet impingement and flow chamber techniques, *Mater. Sci. Eng., C, Biomim. Mater., Sens. Syst.* 26 (2–3) (2006) 260–266.
- [3] J.G. Guan, Y.Q. Miao, Q.J. Zhang, Impedimetric biosensors, *J. Biosci. Bioeng.* 97 (2004) 219–226.
- [4] L. Tamisier, P. Bernabeu, A. De Cesare, A. Caprani, Responses to shear stress and histamine addition of cultured vascular endothelium-kinetic study using electrical impedance measurements, *Electrochim. Acta* 34 (1989) 1339–1350.
- [5] I. Giaever, C.R. Keese, Micromotion of mammalian cells measured electrically, *Proc. Natl. Acad. Sci. U. S. A.* 88 (1991) 7896–7900.
- [6] C. Tiruppathi, A.B. Malik, P.J. Del Vecchio, C.R. Keese, I. Giaever, Electrical method for detection of endothelial cell shape change in real time: Assessment of endothelial barrier function, *Proc. Natl. Acad. Sci. U. S. A.* 89 (1992) 7919–7923.
- [7] I. Giaever, C.R. Keese, Amorphological biosensor for mammalian cells, *Nature* 366 (1993) 591–592.
- [8] I. Giaever, C.R. Keese, use of electric fields to monitor the dynamical aspect of cell behaviour in tissue culture, *IEEE Proc. Biomed. Eng.* 33 (1986) 242–247.
- [9] R. Ehret, W. Baumann, M. Brischwein, A. Shwinde, K. Stegbauer, B. Wolf, Monitoring of cellular behaviour by impedance measurements on interdigitated electrode structures, *Biosens. Bioelectron.* 12 (1997) 29–41.
- [10] J. Wegener, S. Zink, P. RÖen, H.J. Galla, Use of electrical impedance measurements to monitor  $\alpha$ -adrenergic stimulation of bovine aortic endothelial cells, *Eur. J. Physiol.* 437 (1999) 925–934.
- [11] A. Bouaziz, A. Richert, A. Caprani, Vascular endothelial cell responses to different electrically charged poly(vinylidene fluoride) supports under static and oscillating flow conditions, *Biomaterials* 18 (1997) 107–112.
- [12] A. Bouaziz, A. Richert, A. Caprani, Morphological aspects of endothelial cells cultured in absence of foetal calf under controlled electrical charges applied to the support, *Biomaterials* 17 (1996) 2281–2287.
- [13] T. Mossman, Rapid colorimetric assay for cellular growth and survival. Application to proliferation and cytotoxicity assays, *J. Immunol. Methods* 65 (1983) 55–63.
- [14] A. Banan, G.S. Smith, E.R. Kokoska, T.A. Miller, Role of actin cytoskeleton in prostaglandin-induced protection against ethanol in an intestinal epithelial cell line, *J. Surg. Res.* 88 (2) (2000) 104–113.
- [15] Y. Nishiyama, M. Tsuenaga, N. Akutsu, I. Houi, Y. Nakayama, E. Adachi, M. Yamato, T. Hayashi, Dissociation of actin microfilament organization from acquisition and maintenance of elongated shape of human dermal fibroblasts in three dimensional collagen gel, *Matrix* 13 (1993) 447–455.
- [16] K.R. Mendes, R.S. Freire, C.P. Fonseca, S. Neves, L.T. Kubota, Characterization of self-assembled thiols monolayers on gold surface by electrochemical impedance spectroscopy, *J. Braz. Chem. Soc.* 6 (15) (2004) 849–855.
- [17] H. Hillebrandt, A. Abdelghani, C. Abdelghani, E. Sackmann, Electrical and optical characterization of thrombin-induced permeability of cultured endothelial cell monolayers on semiconductor electrode arrays, *Appl. Phys., A* 73 (5) (2001) 539–546.
- [18] Wiegand, PhD thesis: Fundamental principles of the electric properties of supported lipid membranes investigated by advanced methods of impedance spectroscopy, 1999, Shaker verlag, ISBN 3-8265-7231-9, Technische Universität München, Germany.
- [19] R. MacDonald, *Impedance Spectroscopy*, Wiley, New York, 1987.
- [20] S. Hleli, A. Abdelghani, A. Tlili, Impedance spectroscopy Technique for DNA hybridization, *Sensors* 3 (2003) 472–479.
- [21] Ju.J. Zhu, J.Z. Xu, J.T. He, Y.J. Wang, Q. Miao, H.Y. Chen, An electrochemical immunosensors for assays of C-Reactive protein, *Anal. Lett.* 36 (8) (2003) 1547–1556.
- [22] Y. Duvault, A. Gagnaire, F. Gardies, N. Jaffrezic-Renault, C. Martelet, D. Morel, J. Serpinet, J.L. Duvault, Physicochemical characterization of covalently bonded alkyl monolayers on silica surfaces, *Thin Solid Films* 185 (1990) 169–179.
- [23] S. Hleli, C. Martelet, A. Abdelghani, F. Bessueille, A. Errachid, J. Samitier, N. Burais, N. Jaffrezic-Renault, Atrazine analysis using an impedimetric immunosensor based on mixed biotinylated self-assembled monolayer, *Sens. Actuators B* 113 (2006) 711–717.

- [24] H.P. Schwan, in: W.L. Nesluk (Ed.), In determination of biological impedance in physical techniques in research. *Electrophysiological Methods*, Part B, 6, Academic Press, New York, 1963, p. 323.
- [25] M.J. Rutten, R.L. Hooer, M.J. Karnovsky, Electrical resistance and macromolecular permeability of brain endothelial monolayer cultures, *Brain Res.* 425 (2) (1987) 301–310.
- [26] J. Wegener, M. Sieber, H. Galla, Impedance analysis of epithelial and endothelial cell monolayers cultured on gold surfaces, *J. Biochem. Biophys. Methods* 32 (1996) 151–170.
- [27] C. Crone, S.P. Oeson, Electrical resistance of brain microvascular endothelium, *Brain Res.* 241 (1982).
- [28] M.R. Turner, Electrical resistances of cultured bovine arterial endothelium in solutions of various resistivities, *Exp. Physiol.* 741 (1992).
- [29] K.S. Cole, *Membranes, Ions and Impulses*, University of California Press, Berkeley, 1972.
- [30] C. Steinem, A. Janshoff, J. Wegener, W.P. Ulrich, W. Willenbrink, M. Sieber, H.J. Galla, Impedance and shear wave resonance analysis of ligand–recepto interactions at functionalized surfaces and of cell monolayers, *Biosens. Bioelectron.* 12 (1997) 787–808.
- [31] D. Bray, *Cell movements from Molecules to Motility*, 2nd Ed. Garland Publishing Inc., New York, 2001.